

# Quantum Monte-Carlo method applied to Non-Markovian barrier transmission

Guillaume Hupin<sup>1</sup> and Denis Lacroix<sup>1</sup>

<sup>1</sup>*GANIL, Bd Henri Becquerel, BP 55027, 14076 Caen Cedex 5, France*

In nuclear fusion and fission, fluctuation and dissipation arise due to the coupling of collective degrees of freedom with internal excitations. Close to the barrier, both quantum, statistical and non-Markovian effects are expected to be important. In this work, a new approach based on quantum Monte-Carlo addressing this problem is presented. The exact dynamics of a system coupled to an environment is replaced by a set of stochastic evolutions of the system density. The quantum Monte-Carlo method is applied to systems with quadratic potentials. In all range of temperature and coupling, the stochastic method matches the exact evolution showing that non-Markovian effects can be simulated accurately. A comparison with other theories like Nakajima-Zwanzig or Time-ConvolutionLess ones shows that only the latter can be competitive if the expansion in terms of coupling constant is made at least to fourth order. A systematic study of the inverted parabola case is made at different temperatures and coupling constants. The asymptotic passing probability is estimated in different approaches including the Markovian limit. Large differences with the exact result are seen in the latter case or when only second order in the coupling strength is considered as it is generally assumed in nuclear transport models. On opposite, if fourth order in the coupling or quantum Monte-Carlo method is used, a perfect agreement is obtained.

PACS numbers: 24.60-k,25.70.Jj,05.60.Gg

Keywords: open quantum systems, Monte-Carlo methods, non-Markovian effect.

## I. INTRODUCTION

To understand nuclear reactions, the dynamics of nuclei is often replaced by few selected collective degrees of freedom expected to contain important information on the dynamic. This is for instance the case in fusion reactions where the relative distance and/or mass asymmetry is retained [1, 2]. Another example is provided by the fission process which is often treated as a trajectory in an energy landscape function on different deformation parameters [3, 4]. Although the evolution is projected onto few variables, other internal degrees of freedom may play an important role to understand the onset of dissipation or fluctuation phenomena [5]. To treat these effects, the relevant degrees of freedom should be regarded as an Open Quantum System coupled to an environment which simulates the internal dynamics.

To include dissipation in collective space, two important simplifications are often made. First, most of current models treating fusion/fission neglect quantum effects and consider a classical treatment [6–9]. Such an approximation is however expected to be valid only if the internal excitation is high and therefore is not expected to hold close to or below the Coulomb barrier. As it is discussed in ref. [10], a proper treatment of quantum and decoherence effects might be crucial in this region. Second, when the time scale associated to collective dynamics cannot be dissociated from the one of the environment, "non-Markovian" (also called "memory") effect should also be properly treated [11, 12]. Large effort is now devoted to account for both quantal and non-Markovian effects in nuclear reactions [13–18] and more generally in open quantum systems [19].

Recently, the description of open quantum systems by stochastic methods has received much attention [19–

21]. In the Markovian limit, several methods have been proposed to treat fluctuation and dissipation starting from a quantum master equation on the system density [19, 20, 22–28]. These methods have been extended also to treat non-Markovian effects like in Quantum State Diffusion (QSD) [29–32] or quantum Monte-Carlo (QMC) methods [33]. Several groups have shown that these effects could eventually be simulated using Feynman-Vernon influence functional [21, 34] or directly stochastic master equations [35, 36].

In this work, we apply the stochastic formulation proposed in ref. [36] to the case of quadratic potentials coupled to a heat-bath, the so-called Caldeira-Leggett model [37]. The case of inverted potential is the first step towards realistic situations like fusion or fission. The aim of the present work is threefold. First, to introduce the new QMC method and apply it for potentials with barriers similar to those appearing in fusion/fission processes. Second, we show that the exact quantum Monte-Carlo method can be rather accurate to treat the dissipative dynamics of a quantum system. Last, we also present a comparison of this theory with other methods based on projection, namely Nakajima-Zwanzig (NZ) and Time-ConvolutionLess (TCL) [38–41], which are actually widely used to treat non-Markovian effects. Doing so, we show that only TCL up to at least fourth orders in the coupling constant can provide a competitive theory. The paper is organized as follows. In section II, the ingredients and properties of the quantum Monte-Carlo approach are discussed and the link with functional integral is precised. In section III, the method is first illustrated to the case of parabolic potential. Then, the passing probabilities are estimated for the inverted parabola case.

## II. QUANTUM MONTE-CARLO METHOD

Our starting point is a system (S) interacting with a surrounding environment (E). We assume here that the total system (S+E) is described by the Hamiltonian

$$H = H_S + H_E + V. \quad (1)$$

$H_S$  (resp.  $H_E$ ) acts on the system (resp. env.) only while  $V$  induces a coupling between the two sub-systems. Starting from an initial total density  $D(0)$ , the dynamical evolution is given by the Liouville von-Neumann equation on the density:

$$i\hbar \frac{dD(t)}{dt} = [H, D(t)]. \quad (2)$$

In many physical situations, the total number of degrees of freedom to follow in time prevents from solving exactly this equation. One of the leitmotiv of Open Quantum System (OQS) theory is to find accurate approximations for the system evolution without following explicitly irrelevant degrees of freedom associated to the environment and therefore reduces the complexity of the initial problem. Conventional strategy to treat dissipation and fluctuation in an open quantum system is to reduce the information to the system density only  $\rho_S(t) = \text{Tr}_E(D(t))$  while accounting approximately for environment effect. Here, we use a different strategy, the dynamics of the total system is first replaced by a set of stochastic evolutions where the total density remains separable along each path, i.e.  $D = \rho_S(t) \otimes \rho_E(t)$ . Then, the stochastic evolution of the environment is projected onto the relevant degrees of freedom to obtain a closed equation for the system density. It is shown that the new approach provides a proper treatment of dissipation and fluctuation for a system coupled to a surrounding heat-bath.

### A. Quantum Monte-Carlo formulation of Open Quantum Systems

Recently, new stochastic formulations [34, 35, 42, 43] have been developed to study the system+environment problem that avoid evaluation of non-local memory kernels although non-Markovian effects are accounted for exactly (see also [35, 36, 42, 44–47]). One example of such a theory based on quantum Monte-Carlo method is presented here.

Hereafter, it is assumed that the coupling is separable:  $V = Q \otimes B$  where  $Q$  and  $B$  act on the system and environment respectively. For simplicity, initial separable density is considered, i.e.  $D(0) = \rho_S(0) \otimes \rho_E(0)$ . We want to replace the evolution of the total density (Eq. (2)) by an ensemble of stochastic evolutions of both the system and environment such that:

$$\begin{cases} d\rho_S = \frac{dt}{i\hbar} [H_S, \rho_S] + d\xi_S Q \rho_S + d\lambda_S \rho_S Q \\ d\rho_E = \frac{dt}{i\hbar} [H_E, \rho_E] + d\xi_E B \rho_E + d\lambda_E \rho_E B \end{cases} \quad (3)$$

where  $d\xi_{S/E}$  and  $d\lambda_{S/E}$  denote Markovian Gaussian stochastic variables with zero means and where we use Ito convention of stochastic calculus [48]. In the following, we assume in addition that

$$\overline{d\xi_S d\lambda_E} = \overline{d\lambda_S d\xi_E} = 0, \quad (4)$$

where the overline denotes the stochastic average. Along each path, the total density remains separable, i.e.  $D(t) = \rho_S(t) \otimes \rho_E(t)$ . Starting from such a density, at time  $t + dt$ , the average evolution deduced from Eq. (3) is given by

$$\begin{aligned} \overline{dD(t)} &= \frac{dt}{i\hbar} [h_S + h_E, D(t)] \\ &+ \overline{d\xi_S d\xi_E} (Q \otimes B) D(t) + \overline{d\lambda_S d\lambda_E} D(t) (Q \otimes B). \end{aligned}$$

Therefore, under the condition

$$\overline{d\xi_S d\xi_E} = \frac{dt}{i\hbar}, \quad \overline{d\lambda_S d\lambda_E} = -\frac{dt}{i\hbar}, \quad (5)$$

the average evolution over the separable densities that evolve according to Eq. (3) identify with the exact Liouville von Neumann equation of motion (Eq. (2)). The possibility to use simple Gaussian noises to incorporate the environment effect might appear surprising. Indeed, noises used in standard approaches for Open Quantum Systems generally reflect properties of the environment. It should be however kept in mind that such environment dependent noises appear once the environment dynamics has been projected out on the system density evolution. Anticipating the discussion of section II B, once such a projection has been made, the Gaussian noises introduced here, transform into new random variables that explicitly depend on the environment properties.

The discussion above for one time step can then be iterated to show that the exact dynamics of a system+environment could be replaced by an average over an ensemble of stochastic evolutions of separable densities [34–36]. To be really useful, mainly two difficulties should be overcome (i) in general, the environment corresponds to a large number of degrees of freedom that could not be followed explicitly in time. (ii) the numerical implementation of such a theory is possible only if the statistical errors do not grow too fast during the time-evolution. This statistical errors are directly connected to the number of trajectories necessary to accurately describe the physical process. Difficulty (i) is solved in the next section by projecting out the effect of the environment on the system leading to a closed equation for the system density only. Let us first concentrate on statistical errors. At any time, a measure of the statistical fluctuation around the average trajectory is given by

$$\begin{aligned} \Lambda_{stat} &= \overline{\text{Tr} \left\{ \left( D^\dagger(t) - \overline{D^\dagger(t)} \right) \left( D(t) - \overline{D(t)} \right) \right\}} \\ &= \overline{\text{Tr} \left\{ D^\dagger D(t) \right\}} - \overline{\text{Tr} \left\{ \overline{D(t)}^2 \right\}}. \end{aligned} \quad (6)$$

Starting from Eq. (3), the evolution of  $\Lambda_{stat}$  over a small time step reads

$$d\Lambda_{stat} = \frac{2dt}{\hbar} \left\{ \overline{\langle Q^2 \rangle_S} + \overline{\langle B^2 \rangle_E} \right\}, \quad (7)$$

where  $\langle Q^2 \rangle_S \equiv \text{Tr}_S(Q^2 \rho_S(t))$  and  $\langle B^2 \rangle_E \equiv \text{Tr}_E(B^2 \rho_E(t))$ . Statistical errors associated with Eq. (3) have been estimated numerically and turn out to grow very fast in time [46]. As a consequence, the stochastic process in the present form is useless to simulate physical situations and methods to reduce statistical errors should be used.

To do so, it is worth to note that the stochastic equation of motion is not unique. Indeed, any stochastic process of the form:

$$\begin{cases} d\rho_S = \frac{dt}{i\hbar} [H_S + Q\Delta_E, \rho_S] \\ \quad + d\xi_S(Q - \Delta_S)\rho_S + d\lambda_S\rho_S(Q - \Delta_S) \\ d\rho_E = \frac{dt}{i\hbar} [H_E + B\Delta_S, \rho_E] \\ \quad + d\xi_E(B - \Delta_E)\rho_E + d\lambda_E\rho_E(B - \Delta_E) \end{cases}, \quad (8)$$

where  $\Delta_S(t)$  and  $\Delta_E(t)$  are time-dependent parameters leads to the same average evolution. These stochastic equations also provide a reformulation of the initial system+environment problem. Indeed, we have

$$\begin{aligned} \overline{d\rho_S \otimes \rho_E} + \overline{\rho_S \otimes d\rho_E} &= \frac{dt}{i\hbar} [H_S + Q\Delta_E, \rho_S \otimes \rho_E] \\ &\quad + \frac{dt}{i\hbar} [H_E + B\Delta_S, \rho_S \otimes \rho_E] \\ \overline{d\rho_S \otimes d\rho_E} &= \frac{dt}{i\hbar} [(Q - \Delta_S) \otimes (B - \Delta_E), \rho_S \otimes \rho_E]. \end{aligned}$$

Therefore, terms appearing in the deterministic part are exactly compensated by equivalent terms coming from the average over the noise. Accordingly, the evolution of the average density identifies with the exact equation of motion (2).

Up to now, the flexibility has been essentially exploited by using [35, 36]

$$\Delta_E(t) = \langle B(t) \rangle_E, \quad \Delta_S(t) = \langle Q(t) \rangle_S. \quad (9)$$

This choice is justified by the fact that it directly appears when the Ehrenfest theorem is applied to separable total density for system or environment observables. By modifying the stochastic evolution, part of the coupling

is already contained in the deterministic evolution. Accordingly, we do expect that the amount of coupling to be treated by the noise is significantly reduced as well as the statistical errors. In the latter case, statistical fluctuations are given by:

$$d\Lambda_{stat} = \frac{2dt}{\hbar} \left\{ \overline{(\langle Q^2 \rangle_S - \overline{\langle Q \rangle_S^2})} + \overline{(\langle B^2 \rangle_S - \overline{\langle B \rangle_S^2})} \right\} \quad (10)$$

and are always smaller than the original ones (7). As shown numerically in ref. [35], introduction (9) significantly reduces statistical fluctuations and opens new perspectives for the application of the present framework.

The modified stochastic theory has other advantages. For instance, the traces of densities are constant and remain equal to their initial values, i.e.  $d\text{Tr}(\rho_{S/E}) = 0$ . This greatly simplifies expectation values of system and/or environment observables. Indeed, denoting by  $X$  a system operator, along a trajectory, we have

$$\langle X \rangle = \text{Tr}_E(XD(t)) = \text{Tr}(\rho_E(t))\text{Tr}_S(X\rho_S(t)). \quad (11)$$

For stochastic processes with varying trace of densities, the observable evolution will contain terms coming from  $d\text{Tr}(\rho_{S/E})$  and cross terms coming from  $d\text{Tr}(\rho_{S/E})d\text{Tr}(X\rho_S(t))$ . In the case considered here, we simply have

$$d\langle X \rangle = \text{Tr}_E(\rho_E(t))d\text{Tr}_S(X\rho_S(t)). \quad (12)$$

The QMC theory with centered noise overcomes the difficulty (ii) but does not help for (i) since the environment degrees of freedom should still be followed in time. In the next section, we show how irrelevant degrees of freedom can be projected out to obtain a closed stochastic master equation for the system only.

## B. Reduced system density evolution and link with influence-functional theory

The stochastic formulation suffers a priori from the same difficulty as the total dynamics: the environment is in general rather complex and has a large number of degrees of freedom which can hardly be followed in time. In Eq. (8), the influence of the environment on the system only enters through  $\langle B(t) \rangle_E$ . Therefore, instead of following the full environment density evolution, one can concentrate on this observable only. As shown in ref. [43], the second equation in Eqs. (8) can be integrated in time to give:

$$\langle B(t) \rangle_E = \text{Tr}_E(B^I(t - t_0)\rho_E(t_0)) - \frac{1}{\hbar} \int_0^t D(t, s) \langle Q(s) \rangle_S ds - \int_0^t D(t, s) du_E(s) + \int_0^t D_1(t, s) dv_E(s), \quad (13)$$

where  $B^I$  denotes the operator  $B$  written in the interaction picture while  $D$  and  $D_1$  are the memory function given by

$$D(t, s) \equiv i\langle [B(t), B(t-s)] \rangle_E, \quad \text{and} \quad D_1(t, s) \equiv \langle \{B(t), B(t-s)\}_+ \rangle_E - 2\langle B(t) \rangle_E \langle B(t-s) \rangle_E. \quad (14)$$

A new set of stochastic variables  $dv_{S/E}$  and  $du_{S/E}$  have been introduced through  $d\xi_{S/E} = dv_{S/E} - idu_{S/E}$  and  $d\lambda_{S/E} = dv_{S/E} + idu_{S/E}$ , and verify

$$\overline{du_S du_E} = \overline{dv_S dv_E} = \frac{dt}{2\hbar}, \quad \overline{du_S dv_E} = \overline{dv_S du_E} = 0. \quad (15)$$

Reporting the evolution of  $\langle B(t) \rangle_E$  into the evolution of  $\rho_S$ , a closed stochastic equation of motion for the system density is obtained:

$$d\rho_S = \frac{dt}{i\hbar} [H_S, \rho_S] + dt[Q, \rho_S] \int_0^t ds D(t-s) \langle Q(s) \rangle_S + d\xi(t)[Q, \rho_S] + d\eta(t)\{Q - \langle Q \rangle_S, \rho_S\} \quad (16)$$

with

$$d\xi(t) = dt \int_0^t D_1(t-s) dv_E(s) - dt \int_0^t D(t-s) du_E(s) - idv_S(t), \quad d\eta(t) = du_S(t). \quad (17)$$

By integrating out the evolution of the environment, a new stochastic term is found that depends not only on the noise at time  $t$  but also on its full history through the time integrals. Using second moments given by Eqs. (15) leads to:

$$\begin{aligned} \overline{d\eta(t)d\eta(t')} &= 0, \\ \overline{d\xi(t)d\eta(t')} &= -\frac{dt}{2\hbar}\Theta(t-t')D(t-t'), \\ \overline{d\xi(t)d\xi(t')} &= -\frac{idt}{2\hbar}D_1(|t-t'|), \end{aligned}$$

where  $\Theta(t-t') = 1$  if  $t > t'$  and 0 elsewhere. Interestingly enough, the stochastic equation given by (16) identifies with the stochastic master equation obtained in ref. [21] using a completely different method based on the Feynman-Vernon influence functional theory [49]. It should however be kept in mind that different strategies to design the stochastic equation (see discussion in section II A) would have given a different stochastic master equation.

Despite the apparent complexity of Eq. (16), the QMC approach has been recently applied with success to the spin-boson model coupled to a heat bath of oscillators [43]. In particular, the introduction of (9) seems to cure the numerical difficulties that have been encountered in this model [46]. By projecting the environment effect onto the system density evolution we do not need anymore to follow the environment density and we expect that a rather limited number of trajectories will be sufficient to accurately simulate the onset of dissipation and fluctuation in an open quantum system. Eq. (16) is the equation that is solved in practice. It should be noted that the present stochastic process differs significantly from conventional approaches. Indeed, according to the noise properties, system densities are non-

hermitian along a stochastic path. As a consequence, expectation value of observables are complex losing their physical meaning before averaging over the stochastic path. Nevertheless, we illustrate in the following that the new theory can be a very powerful tool.

### III. APPLICATION

The Caldeira-Leggett (CL) model [37] corresponds to a single harmonic oscillator coupled to an environment of harmonic oscillators initially at thermal equilibrium, i.e.

$$H_S = H_c + \frac{P^2}{2M} + \varepsilon \frac{1}{2} M \omega_0^2 Q^2, \quad (18)$$

$$H_E = \sum_n \left( \frac{p_n^2}{2m_n} + \frac{1}{2} m_n \omega_n^2 x_n^2 \right) \quad (19)$$

and  $B \equiv -\sum_n \kappa_n x_n$  [19]. Here,  $H_c = Q^2 \sum_n \frac{\kappa_n^2}{2m_n \omega_n^2}$  is the counter-term that insures that the physical frequency is  $\omega_0$ . In the following,  $\varepsilon$  is either +1 (harmonic case) or -1 (inverted parabola case). Such a model can be solved exactly.

As shown in ref. [43], the two functions  $D$  and  $D_1$  defined by Eqs. (14) and estimated along the stochastic trajectories identify with the standard times correlation functions:

$$D(\tau) = 2\hbar \int_0^{+\infty} d\omega J(\omega) \sin(\omega\tau), \quad (20)$$

$$D_1(\tau) = 2\hbar \int_0^{+\infty} d\omega J(\omega) \coth(\hbar\omega/2k_B T) \cos(\omega\tau) \quad (21)$$

where  $J(\omega) \equiv \sum_n \frac{\kappa_n^2}{2m_n \omega_n} \delta(\omega - \omega_n)$  denotes the spectral

density characteristic of the environment [19, 50]. In the following, a Drude spectral density [43]

$$J(\omega) = \frac{2M\eta}{\pi} \omega \frac{\Omega^2}{\omega^2 + \Omega^2}, \quad (22)$$

is considered where  $M$  is the nucleon mass.

### A. Quantum Monte-Carlo method for parabolic potentials

As a first illustration, the harmonic case ( $\varepsilon = +1$ ) is considered. This case has been already studied in ref. [51] using the stochastic method proposed in ref. [21]. In the CL model, starting from an initial Gaussian density, the system density remains gaussian along the stochastic path. Therefore, the stochastic evolution of the system density reduces to the first and second moments evolution of  $\langle P \rangle$  and  $\langle Q \rangle$  given by [36]:

$$\begin{cases} d\langle Q \rangle = \frac{\langle P \rangle}{M} dt + 2du_S \sigma_{QQ} \\ d\langle P \rangle = -M\omega_0^2 \langle Q \rangle dt - dt \langle B \rangle + 2du_S \sigma_{PQ} - \hbar dv_S \\ d\sigma_{QQ} = 2\frac{dt}{M} \sigma_{PQ} \\ d\sigma_{PP} = -2M\omega_0^2 dt \sigma_{PQ} \\ d\sigma_{PQ} = \frac{dt}{M} \sigma_{PP} - M\omega_0^2 \sigma_{QQ} dt \end{cases} \quad (23)$$

These equations illustrate the differences between the new exact reformulation and standard methods to treat dissipation. Generally, the noise enters into the evolution of  $\langle P \rangle$  only and affects directly the second moment. Here, we see that second moments identify with the unperturbed ones while the random forces enter in both  $\langle Q \rangle$  and  $\langle P \rangle$ . In addition, the noise is complex, which implies that observables make excursions into the complex plane. This stems from the specific noise used to design the exact formulation that leads to non-Hermitian densities along paths. Part of the conceptual difficulties in understanding the physical meaning of observable evolutions can be overcome by noting that if  $\rho_S(t)$  belongs to the set of trajectories, by symmetry  $\rho_S^\dagger(t)$  will also belong to the set. By grouping these two trajectories to estimate observables, real quantities are deduced.

The exact evolution is obtained by averaging over different trajectories. For second moments, this leads to

$$\Sigma_{QQ} \equiv \overline{\langle Q^2 \rangle} - \overline{\langle Q \rangle}^2 = \sigma_{QQ} + \overline{\langle Q \rangle^2} - \overline{\langle Q \rangle}^2 \quad (24)$$

where  $\overline{\langle X \rangle}$  denotes the statistical average of quantum expectation values  $\langle X \rangle$ . It is a particularity of the CL model that total fluctuation is recovered by simply adding up quantum and statistical fluctuations.

An example of  $\Sigma_{QQ}(t)$  evolution obtained using Eq. (24) (red filled circles) is compared to the exact result (solid line) in figure 1. As an indication, the evolution of

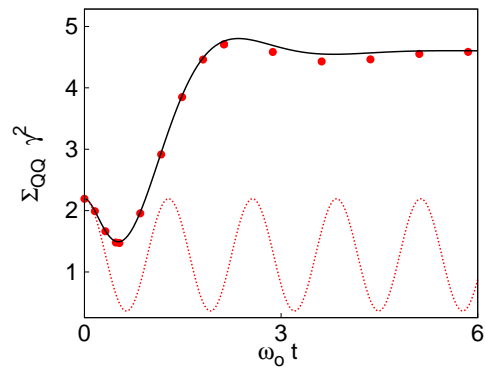


FIG. 1: (Color online) Evolution of  $\Sigma_{QQ}$  (filled circles) obtained by averaging over  $10^5$  trajectories. This evolution is compared to the exact result (solid line) and to the quantum fluctuation  $\sigma_{QQ}$  evolution (dotted line). Parameters of the simulation are  $k_B T = \hbar\omega_0$ ,  $\hbar\Omega = 5\hbar\omega_0$ ,  $\eta = 0, 5\hbar\omega_0$  and  $\hbar\omega_0 = 14MeV$ . The factor  $\gamma$  defined as  $\gamma^2 = \hbar/(2M\omega_0)$  equals here  $\gamma = 1.216 \text{ fm}^{-1}$ .

quantum fluctuation  $\sigma_{QQ}$ , which is identical for all trajectories, is also displayed (dotted line). Note that, Eq. (16) is already exact for the evolution of first moments  $\langle P \rangle$  and  $\langle Q \rangle$ , even if the noise is omitted. However, it completely fails to account for fluctuation. While the quantum evolution does not present any damping, the average evolution closely follows the exact solution. The harmonic oscillations in  $\sigma_{QQ}$  are due to the fact that the width of the initial density differs from the width of the coherent state associated to the considered oscillator, i.e.  $\sigma_{QQ}(0) \neq \hbar/(2M\omega_0)$ . This is at variance with the simulation made in ref. [51].

The accuracy of the quantum Monte-Carlo theory has been systematically investigated for various temperatures and coupling strengths. In all cases, averaged evolutions could almost not be distinguished from the exact evolution. This is illustrated in figure 2 where  $\Sigma_{QQ}$  (left),  $\Sigma_{PP}$  (middle) and  $\Sigma_{PQ}$  (right) are displayed as a function of time and compared to exact solutions for various temperatures. Figure 2, clearly shows that the stochastic method properly includes all non-Markovian effects. In particular at low temperature, typically  $k_B T < \hbar\omega_0$ , and medium coupling constant  $\eta$ , large memory effect is expected.

### B. Application of NZ and TCL

Conjointly to the benchmark of quantum Monte-Carlo approaches, we also tested projection method either based on the Nakajima-Zwanzig [19, 38, 39, 52] or Time ConvolutionLess [19, 40, 41, 52] formalisms. Both theories provide *a priori* exact re-formulations of the initial problem and lead to a closed master equation for the system density. However, they differ completely in the strategy and equation of motion used to incorporate memory

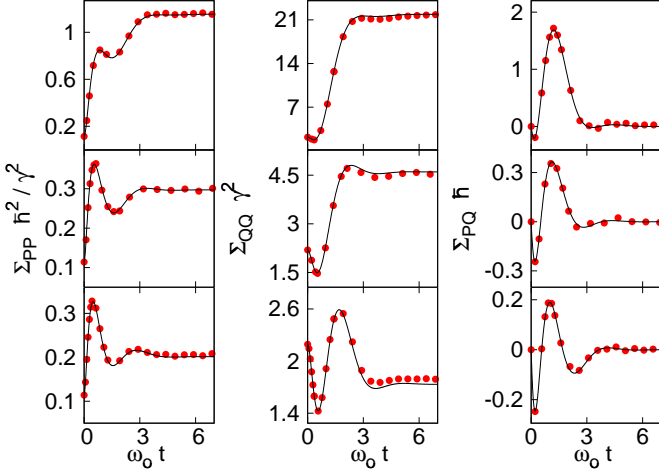


FIG. 2: (Color online) Evolution of  $\Sigma_{PP}$  (left),  $\Sigma_{QQ}$  (middle) and  $\Sigma_{PQ}$  (right) obtained with  $10^5$  trajectories are displayed with red filled circles as a function of time and systematically compared with the exact evolution (solid line).  $k_B T = 5\hbar\omega_0$ ,  $\hbar\omega_0$  and  $0, 1\hbar\omega_0$  are respectively shown from top to bottom. In all cases,  $\eta = 0, 5\hbar\omega_0, \hbar\Omega = 5\hbar\omega_0$  and  $\hbar\omega_0 = 14MeV$ .

effects. In the NZ case, the evolution of the system density at time  $t$  depends on its full history (i.e. on  $\rho_S(s)$  for all  $s \leq t$ ). In the TCL case, the master equation is local in time and non-Markovian effects are treated in time-dependent transport coefficients. To illustrate the differences between our new QMC method and TCL, we remind below the corresponding local master equation, for  $V = Q \otimes B$ .

$$\begin{aligned} \hbar \frac{d}{dt} \rho_S(t) = & -i[H_S, \rho_S(t)] - \frac{i}{2} \Delta(t) [Q, \{Q, \rho_S(t)\}] \\ & - 2i\lambda(t) [Q, \{P, \rho_S(t)\}] - \frac{D_{PP}(t)}{\hbar} [Q, [Q, \rho_S(t)]] \\ & + 2 \frac{D_{PQ}(t)}{\hbar} [Q, [P, \rho_S(t)]]. \end{aligned} \quad (25)$$

$\Delta(t)$ ,  $\lambda(t)$ ,  $D_{PQ}(t)$  and  $D_{PP}(t)$  are time-dependent transport coefficients that contain memory effects. Similarly to the QMC case, the solution of the master Eq. (25) is equivalent to follow first and second moments

given by:

$$\left\{ \begin{aligned} \frac{d\langle Q \rangle}{dt} &= \frac{\langle P \rangle}{M} \\ \frac{d\langle P \rangle}{dt} &= -M\omega_p^2(t) \langle Q \rangle - 2\lambda(t) \langle P \rangle \\ \frac{d\Sigma_{PP}}{dt} &= -2M\omega_p^2(t) \Sigma_{PQ} - 4\lambda(t) \Sigma_{PP} + 2D_{PP}(t) \\ \frac{d\Sigma_{QQ}}{dt} &= 2 \frac{\Sigma_{PQ}}{M} \\ \frac{d\Sigma_{PQ}}{dt} &= -M\omega_p^2(t) \Sigma_{QQ} - 2\lambda(t) \Sigma_{PQ} \\ &+ \frac{\Sigma_{PP}}{M} + 2D_{PQ}(t) \end{aligned} \right. ,$$

with  $\omega_p^2(t) = \omega_0^2 + \Delta(t)$ . In practice, the exact NZ or TCL theory cannot be exactly solved and an expansion in powers of the coupling constant is made. In the following, NZ2 (or TCL2) will refer to the expansion up to second order while NZ4 (or TCL4) will refer to the expansion is made up to fourth order. By neglecting higher orders in the coupling in NZ2 (resp. TCL2) or NZ4 (resp. TCL4), both theory are not exact anymore. In the following, the efficiency of each method is systematically discussed.

In Figure 3, the evolution of  $\Sigma_{PP}$  for different cut-off frequencies  $\hbar\Omega$  and coupling strengths  $\eta$  are compared to the exact evolution (solid line). Explicit forms of the equation of motion in the NZ and TCL case can be respectively found in ref. [19, 38, 39, 52] and [19, 40, 41, 52]. Several important remarks could be drawn from this comparison: (i) In all cases, when the coupling strength is considered up to second order, NZ2 (open triangles) provides a better approximation than TCL2 (open squares). This might indeed be expected since NZ2 and TCL2 are respectively equivalent to the Born and Redfield master equation and the former contains a priori less approximations than the latter. (ii) While the TCL4 (filled squares) leads to a clear improvement compared to the TCL2, NZ4 (filled triangles) is in general worse than NZ2. This is a known difficulty of NZ approach and was one of the motivation for the introduction of TCL method (see discussion in ref. [19, 40, 41]). This stems from the fact that the order in perturbation in NZ cannot be identified. For instance, NZ2 (resp. NZ4) contains orders in coupling constant greater than 2 (resp. 4). As a result, the NZ theory does not lead to better results when the "apparent" order in the coupling increases. The TCL method essentially cures this pathology and precise orders in the coupling can be selected. (iii) Rather large deviations between the exact and TCL2 are observed for different cut-off frequencies and coupling strengths. This issue is important since several theories have been recently developed along the line of TCL2 to include memory effects in fusion and fission reactions [14, 15, 17]. Note that, the accuracy of TCL2 depends on different parameters used in the spectral density, in particular of the parameter  $\hbar\Omega$ . Here,

we have used a value of the cut-off frequency between 10 and 20 MeV, which gives realistic dissipation and fluctuation for the fusion or fission mechanism[14, 15, 18]. Our study clearly points out that a proper treatment of memory requires to include higher order effects. (iv) Finally, in all cases, TCL4 could not be distinguished from the exact result. As we will see, the efficiency of TCL4 is similar for the inverted parabola.

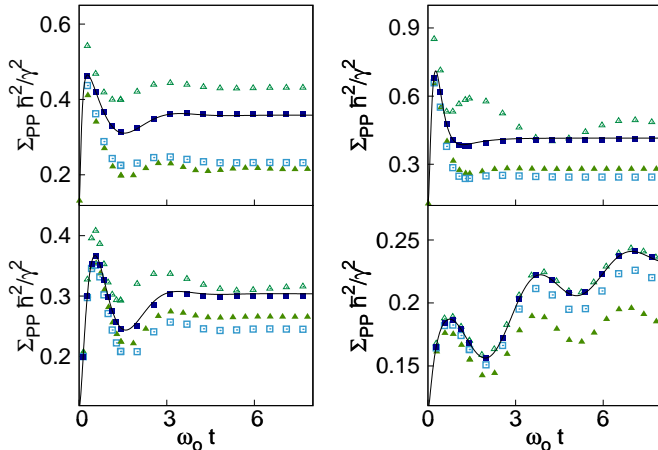


FIG. 3: (Color online) Evolution of  $\Sigma_{PP}$  for different approximations: NZ2 (open triangles), NZ4 (filled triangles), TCL2 (open squares) and TCL4 (filled squares). The exact evolution is displayed with solid line. In all cases,  $\hbar\omega_0 = 14$  MeV, and  $k_B T = \hbar\omega_0$  are used. The left side, corresponds to different cut-off frequencies:  $\hbar\Omega = 20\hbar\omega_0$  (top) and  $\hbar\Omega = 5\hbar\omega_0$  (bottom). In both cases,  $\eta = 0, 5\hbar\omega_0$ . In the right side,  $\hbar\Omega = 10\hbar\omega_0$  and different coupling strengths are used:  $\eta = \hbar\omega_0$  (top) and  $\eta = 0.1\hbar\omega_0$  (bottom).

Since NZ method is not competitive, only the quantum Monte-Carlo and TCL methods are considered in the following application.

### C. Quantum Monte-Carlo method applied to inverted oscillators

Several approaches have been recently developed to describe fusion and fission reactions [6, 14, 15, 17, 18, 53]. In these mechanisms, few collective degrees of freedom couple to a sea of internal excitations while passing an inverted barrier. At very low energy, both quantum and non-Markovian effects are expected to play a significant role. Most of the theory currently used start from quantum master equations deduced from TCL2. The quantum Monte-Carlo method offers a practical alternative which has similarities with path integrals theory. Path integrals are known to provide a possible framework to include dissipation while passing barriers (see for instance [54]). However, due to their complexity, only few applications have been made so far [2, 55]. We compare here the different approaches for inverted potential ( $\varepsilon = -1$ ).

#### 1. Initial conditions, trajectories and mean evolution

Initially, we consider a Gaussian density with quantum width  $\sigma_{QQ}(0) = 0.16$  fm<sup>2</sup> and  $\sigma_{PQ}(0) = 0$  MeV.fm/c and positioned on one side of the potential (here taken arbitrarily at  $\langle Q(0) \rangle = Q_0 > 0$  while the barrier height is located at 0 fm and is by convention taken as  $V_B = 0$  MeV). The initial kinetic energy, denoted  $E_K(0)$  is set by boosting the density with an initial momentum  $\langle P(0) \rangle = P_0 < 0$ .

Contrary to the classical theory of Brownian motion, the notion of trajectories is not so easy to tackle in the present Monte-Carlo framework. First, observables are complex. As mentioned in section III A, this difficulty can be overcome by grouping trajectories by pairs which is equivalent to replace expectation of observables by their real parts. Second, it should be kept in mind that the present theory is a purely quantum theory where densities associated to wave-packets are evolved. Therefore, each trajectory should be interpreted in the statistical sense of quantum mechanics and contains many classical paths. Nevertheless, to visualize the trajectory we define the following energies:

$$E(t) = \frac{P(t)^2}{2m} - \frac{1}{2}m\omega_0^2 Q(t)^2 \quad (26)$$

where  $Q(t)$  and  $P(t)$  denote the real part of  $\langle Q(t) \rangle$  and  $\langle P(t) \rangle$  along the trajectory. An illustration of two trajectories, one passing the barrier and one reflected is shown in figure 4. As illustrated in the following, it is convenient to group trajectories according to the quantity  $\Delta E$  defined by

$$\Delta E = E(0) - V_B \quad (27)$$

which is nothing but the difference between total initial energy and barrier high. Both trajectories shown in figure 4 correspond to  $\Delta E = 0$  MeV.

It is tempting to group trajectories into those passing the barrier and those reflected by the potential to get information on the passing probability or passing time, however, it should be kept in mind that the present theory is fully quantal. Since each trajectories are associated with densities with quantum widths, both trajectories presented in Fig. 4 contribute to the transmission probability.

The accuracy of different methods is illustrated in figure 5 where evolutions of  $\langle Q \rangle$ ,  $\langle P \rangle$ ,  $\Sigma_{QQ}$  and  $\Sigma_{PP}$  are shown as a function of time. Values of parameters retained for this figure are typical values generally taken in the nuclear context[16]. In all cases, including TCL2, second moments are well reproduced. However, only TCL4 and the stochastic simulation provides a correct description of first moments. Calculations are shown here for  $\Delta E = 0$  MeV. TCL2 provides a better and better approximation when  $\Delta E$  increases while the disagreement increases below the barrier. This will be further illustrated below.

## D. Transmission probability

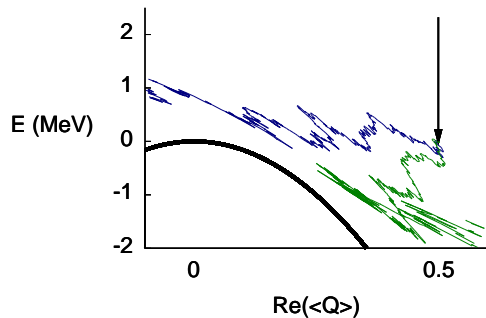


FIG. 4: (Color online) Evolution of  $E(t)$  as a function of  $Q(t)$  for two trajectories (dark and bright lines) with  $\Delta E = 0$  MeV,  $k_B T = 1$  MeV and  $\eta = 0.003$  MeV. The black arrow indicates the initial position of the trajectories while the potential is also shown with bold line as a reference.

Different coupling parameters, cut-off frequencies and temperatures have been investigated showing that both TCL4 and quantum Monte-Carlo are very accurate theories leading always to results on top of the exact ones. It should be noted that the number of trajectories used in the stochastic approach to get small statistical errors is rather small (around  $10^5$ ) which is quite encouraging for future applications.

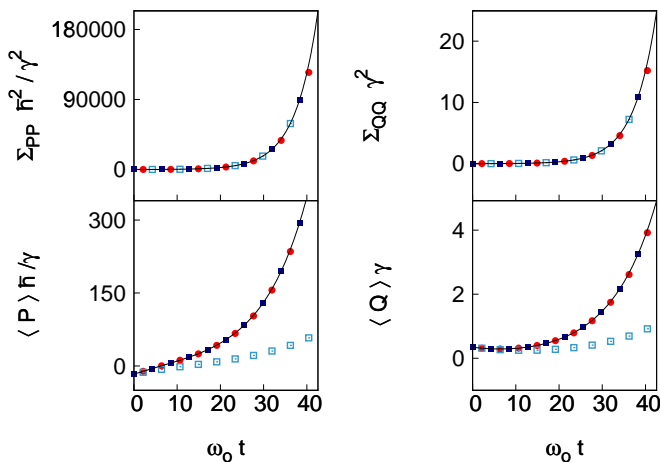


FIG. 5: (Color online) Evolution of  $\langle Q \rangle$ ,  $\langle P \rangle$ ,  $\Sigma_{QQ}$  and  $\Sigma_{PP}$  as a function of time obtained with quantum Monte-Carlo (filled circles), TCL2 (open squares) and TCL4 (filled squares). The exact evolution is also displayed with a solid line. Parameters of the simulations are  $V_B = 4$  MeV,  $\hbar\omega_0 = 1$  MeV,  $\eta = 0.03$  MeV,  $\hbar\Omega = 15\hbar\omega$ ,  $k_B T = 1$  MeV,  $\Delta E = 0$  MeV and  $\gamma = 0.402$  fm $^{-1}$ .  $10^5$  trajectories have been used for the quantum Monte-Carlo case.

The accuracy of the method used to incorporate non-Markovian effects directly affects the predicting power of the theory. This aspect is illustrated here with the passing probabilities. Such a probability is a crucial ingredient in particular for models dedicated to the formation of very heavy elements [7, 14, 15, 17, 53, 56, 57] and should be precisely estimated.

The asymptotic passing probability is usually defined as:

$$P(+\infty) = \lim_{t \rightarrow +\infty} \frac{1}{2} \operatorname{erfc} \left( -\frac{|q(t)|}{\sqrt{2\sigma_{qq}(t)}} \right). \quad (28)$$

where  $q(t)$  and  $\sigma_{qq}(t)$  denote the expectation value and second moment of  $Q$  deduced from the considered theory. In the quantum Monte-Carlo case, these quantities identify with  $\overline{\langle Q(t) \rangle}$  and  $\Sigma_{QQ}(t)$  respectively. To quantify the precision of each theory, we have systematically investigated the difference between the estimated passing probability and the exact one using the parameter  $\Delta P/P$ :

$$\frac{\Delta P}{P} \equiv \frac{P(+\infty) - P_{ex}(+\infty)}{P_{ex}(+\infty)} \quad (29)$$

where  $P(+\infty)$  and  $P_{ex}(+\infty)$  denote the results of the specific calculation considered and the exact one respectively. Figure 6 presents the evolution of  $\Delta P/P$  as a function of  $\Delta E$  obtained for different coupling strengths and temperatures for the quantum Monte-Carlo (filled circles), TCL2 (open squares), TCL4 (filled squares) cases. In this figure, the Markovian approximation is also shown by open crosses.

Once again, the TCL4 and the quantum Monte Carlo methods are in perfect agreement with the exact solution for any input parameters. Small differences sometimes observed between the stochastic approach and the exact value come from the limited number of trajectories used to obtain figure 6. Well above the barrier (here at least two times), TCL2 converges towards the exact case. However, at low  $\Delta E$ , it turns out to be a rather poor approximation. The difference seen in the TCL2 case can directly be traced back to the discrepancy already observed in figure 5 and further confirms the difficulty of treating non-Markovian effects below the barrier. We can see that at lowest energy considered here, the error could be as large as 20% in the weak coupling case and more than 100% in the strong coupling limit. It is worth finally to mention that below the barrier, the Markovian limit gives an even better result than the TCL2 case.

## IV. SUMMARY AND DISCUSSION

In this work, the quantum Monte-Carlo approach recently proposed in ref. [43] to incorporate exactly non-Markovian effects is introduced and applied to the case of harmonic potentials coupled to a heat-bath.

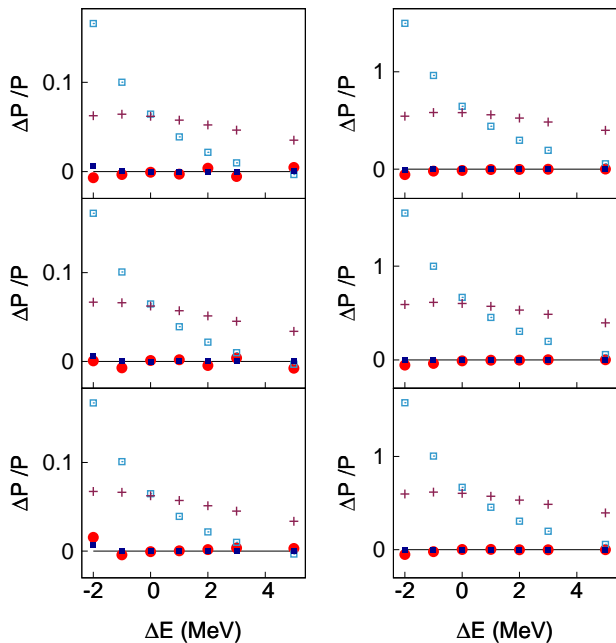


FIG. 6: (Color online) Evolution of  $\Delta P/P$  as a function of  $\Delta E$  calculated using quantum Monte-Carlo (filled circles), TCL2 (open squares), TCL4 (filled squares) and Markovian approximation (open crosses) for different coupling constant:  $\eta = 0.003 \text{ MeV}$  (left) and  $\eta = 0.03 \text{ MeV}$  (right). In both cases,  $T = 5\hbar\omega$ ,  $\hbar\omega$  and  $0, 1\hbar\omega$  are shown from top to bottom.

For both non-inverted and inverted potentials, the new technique is rather effective to reproduce the exact evolution with a rather limited numbers of trajectories.

Other methods have also been benchmarked. The TCL2 method, which is now widely used in nuclear physics to estimate passing probabilities, turns out to deviate significantly from the expected result especially below the barrier and even in the weak coupling regime. To properly treat the dynamics of barrier transmission, higher orders in the coupling strength should be incorporated. TCL4 gives very good agreement with the exact evolution in all cases considered here. The conclusion of our present work is that both quantum Monte-Carlo approach and TCL4 could be considered as good candidates to include memory effects for situations of interest in nuclear physics. Henceforth, the TCL2 method which is widely used nowadays should be replaced by TCL4. The possibility to use stochastic formulation that are exact in average open new perspectives to describe a system coupled to a complex environment. The application to harmonic potential gives interesting insight into such a theory. Application to more general potential turns out to be less straightforward with the appearance of spikes which have been already observed in several formalism where non linear stochastic equations appear [28]. To make these theories more versatile, new methods like the one proposed recently in ref. [58] could be used.

### Acknowledgments

We thanks D.Boilley for his careful reading of the manuscript and G.Adamian and N.Antonenko for fruitful discussions.

- 
- [1] W. U. Schröder and J. R. Huizenga, *Treatise on Heavy-Ion Science* **3**, 115 (1984).
  - [2] P. Fröbrich and R. Lipperheide, *Theory of nuclear reactions* (Oxford University Press, 1996).
  - [3] J. F. Berger, M. Girod, and D. Gogny, *Nucl. Phys. A* **428**, 23 (1984).
  - [4] P. Möller and S. G. Nilsson, *Phys. Lett. B* **31**, 283 (1970).
  - [5] Y. Abe, S. Ayik, P.-G. Reinhard, and E. Suraud, *Phys. Rep.* **275**, 49 (1996).
  - [6] Y. Aritomo, T. Wada, M. Ohta, and Y. Abe, *Phys. Rev. C* **59**, 796 (1999).
  - [7] Y. Abe, D. Boilley, B. G. Giraud, and T. Wada, *Phys. Rev. E* **61**, 1125 (2000).
  - [8] Y. Abe, *Eur. Phys. J. A* **13**, 143 (2002).
  - [9] C. Shen, G. Kosenko, and Y. Abe, *Phys. Rev. C* **66**, 061602 (2002).
  - [10] A. Diaz-Torres, D. J. Hinde, M. Dasgupta, G. J. Milburn, and J. A. Tostevin, *Phys. Rev. C* **78**, 064604 (2008).
  - [11] D. Boilley and Y. Lallouet, *J. of Stat. Phys.* **125**, 473 (2006).
  - [12] S. Matsumoto and M. Yoshimura, *Phys. Rev. A* **63**, 012104 (2000).
  - [13] C. Rummel and H. Hofmann, *Nucl. Phys. A* **727**, 24 (2003).
  - [14] N. Takigawa, S. Ayik, K. Washiyama, and S. Kimura, *Phys. Rev. C* **69**, 054605 (2004).
  - [15] S. Ayik, B. Yilmaz, A. Gokalp, O. Yilmaz, and N. Takigawa, *Phys. Rev. C* **71**, 054611 (2005).
  - [16] V. Sargsyan, Y. Palchikov, Z. Kanokov, G. Adamian, and N. Antonenko, *Physica A* **386**, 36 (2007).
  - [17] K. Washiyama, N. Takigawa, and S. Ayik, in *AIP Conference Proceedings* (2007), vol. 891, p. 413.
  - [18] V. V. Sargsyan, Z. Kanokov, G. G. Adamian, and N. V. Antonenko, *Phys. Rev. C* **77**, 024607 (2008).
  - [19] H. Breuer and F. Petruccione, *The Theory of Open Quantum Systems* (Oxford University Press, Oxford, 2002).
  - [20] M. B. Plenio and P. L. Knight, *Rev. Mod. Phys.* **70**, 101 (1998).
  - [21] J. T. Stockburger and H. Grabert, *Phys. Rev. Lett.* **88**, 170407 (2002).
  - [22] J. Dalibard, Y. Castin, and K. Mølmer, *Phys. Rev. Lett.* **68**, 580 (1992).
  - [23] R. Dum, P. Zoller, and H. Ritsch, *Phys. Rev. A* **45**, 4879 (1992).

- [24] N. Gisin and I. Percival, *J. Phys. A* **25**, 5677 (1992).
- [25] H. Carmichael, *An Open Systems Approach to Quantum Optics* (Lecture Notes in Physics, Springer-Verlag, Berlin, 1993).
- [26] Y. Castin and K. Mølmer, *Phys. Rev. A* **54**, 5275 (1996).
- [27] M. Rigo and N. Gisin, *Quantum Semiclass. Opt.* **8**, 255 (1996).
- [28] W. Gardiner and P. Zoller, *Quantum Noise* (Springer-Verlag, Berlin-Heidelberg, 2000).
- [29] W. T. Strunz, *Phys. Lett. A* **224**, 25 (1996).
- [30] L. Diósi, N. Gisin, and W. T. Strunz, *Phys. Rev. A* **58**, 1699 (1998).
- [31] W. T. Strunz, L. Diósi, and N. Gisin, *Phys. Rev. Lett.* **82**, 1801 (1999).
- [32] W. T. Strunz, *New Journ. of Phys.* **7**, 91 (2005).
- [33] J. Piilo, S. Maniscalco, K. Härkönen, and K.-A. Suominen, *Phys. Rev. Lett.* **100**, 180402 (2008).
- [34] J. Shao, *J. Chem. Phys.* **120**, 5053 (2004).
- [35] D. Lacroix, *Phys. Rev. A* **72**, 013805 (2005).
- [36] D. Lacroix and G. Hupin, Proceedings of "FUSION08: New Aspects of Heavy Ion Collisions near the Coulomb Barrier", September 22-26, 2008, Chicago, USA (2008).
- [37] A. O. Caldeira and A. J. Leggett, *Ann. Phys.* **149**, 374 (1983).
- [38] S. Nakajima, *Prog. Theor. Phys.* **20**, 948 (1958).
- [39] R. Zwanzig, *J. Chem. Phys.* **33**, 1341 (1960).
- [40] F. Hashitsume, N. Shibata and M. Shingū, *J. Stat. Phys.* **17**, 155 (1977).
- [41] F. Shibata, Y. Takahashi, and N. Hashitsume, *J. Stat. Phys.* **17**, 171 (1977).
- [42] H.-P. Breuer, *Eur. Phys. J. D* **29**, 105 (2004).
- [43] D. Lacroix, *Phys. Rev. E* **77**, 041126 (2008).
- [44] H.-P. Breuer, D. Burgarth, and F. Petruccione, *Phys. Rev. B* **70**, 045323 (2004).
- [45] H.-P. Breuer, *Physical Review A* **69**, 022115 (2004).
- [46] Y. Zhou, Y. Yan, and J. Shao, *Eur. Phys. Lett.* **3**, 334 (2005).
- [47] H.-P. Breuer and F. Petruccione, *Phys. Rev. E* **76**, 016701 (2007).
- [48] W. Gardiner, *Handbook of Stochastic Methods* (Springer-Verlag, Berlin-Heidelberg, 1985).
- [49] R. P. Feynman and F. L. Vernon, *Ann. Phys.* **24**, 118 (1963).
- [50] A. J. Leggett, S. Chakravarty, A. T. Dorsey, M. P. A. Fisher, A. Garg, and W. Zwerger, *Rev. Mod. Phys.* **59**, 1 (1987).
- [51] J. T. Stockburger and H. Grabert, *Chem. Phys.* **268**, 249 (2001).
- [52] J. Gemmer and H.-P. Breuer, *Eur. Phys. J. ST* **151**, 1 (2007).
- [53] D. Boilley, Y. Abe, and J. Bao, *Eur. Phys. J. A* **18**, 627 (2003).
- [54] A. O. Caldeira and A. J. Leggett, *Phys. Rev. Lett.* **46**, 211 (1981).
- [55] P. Fröbrich, R. Lipperheide, and K. Möhring, *Zeitschrift für Physik B Condensed Matter* **78**, 325 (1990).
- [56] J.-D. Bao and D. Boilley, *Nucl. Phys. A* **707**, 47 (2002).
- [57] B. Yilmaz, S. Ayik, Y. Abe, and D. Boilley, *Phys. Rev. E* **77**, 011121 (2008).
- [58] W. Koch, F. Großmann, J. T. Stockburger, and J. Ankerhold, *Phys. Rev. Lett.* **100**, 230402 (2008).